CSMA 2017
13ème Colloque National en Calcul des Structures
15-19 Mai 2017, Presqu'île de Giens (Var)

# 3D Full field modelling of recrystallization in a finite element framework – application to 304L

L. Maire[1], B. Scholtes[1,2], C. Moussa[1], N. Bozzolo[1], A. Settefrati[2], I. Poitrault[3], A. Karch[1], M. Bernacki[1]

[1] *MINES ParisTech, PSL - Research University, CEMEF - Centre de mise en forme des matériaux, CNRS UMR 7635, CS 10207 rue Claude Daunesse 06904 Sophia Antipolis Cedex, France.*
[2] *Transvalor SA, 694 avenue Docteur Maurice Donat, 06250 Mougins, France.*
[3] *Industeel, ArcelorMittal, CRMC 71200 Le Creusot, France.*

**Résumé** — This paper describes a level-set framework for the full field modelling of recrystallization and grain growth in a polycrystalline material. Topological evolutions are simulated based on a kinetic law linking the velocity of the boundaries to the thermodynamic driving forces. Dynamic recrystallization is also modelled by coupling the level-set method to mean field laws describing strain hardening mechanism and nucleation criteria. The proposed formalism enables to reach outstanding massively multi-domain computations in a front-capturing finite element framework comparatively to the state of art.

**Mots clés** — full field, mean field, recrystallization.

## 1 Introduction

The mechanical and thermal properties of metallic materials are strongly related to their microstructure. The understanding and the modelling of the microstructural evolution mechanisms is then crucial when it comes to optimize the forming process and the final in-use properties of the materials. Macroscopic and homogenized models, also called mean-field models are widely used in the industry, mainly due to their low computational cost. They are generally based on empirical laws and thus require many fitting parameters which must be calibrated through experimental testing or lower-scale simulations. Furthermore, given the complexity of modern metallurgical problems, these models may not be accurate enough to capture local but significant events. Thanks to the explosion of computer capacities, finer modelling techniques are now available. These lower scale approaches, the so-called full field models, are based on a full description of the microstructure topology [1, 2]. They have demonstrated an interesting potential for the modelling of complex mechanisms, such as abnormal grain growth or Zenner-pinning phenomena, which are hardly predicted with homogenized approaches. Over the last decades, several mesoscale numerical models have been developed to simulate the microstructure evolution due to recrystallization (ReX). Probabilistic voxel-based approaches such as Monte Carlo [3] and Cellular Automata [4] are very popular. There are also deterministic approaches which enable to avoid probabilistic laws but are more greedy in terms of computational resources due to the fact that they involve the solving of large systems of partial differential equations. Thus several workers have developed the vertex method [5] wherein the grain boundaries are defined in terms of vertices ; the interface motion is then imposed by the displacement of a set of points. Another approach found in the literature is the phase-field method, which offers the advantage of avoiding the difficult problem of tracking interfaces [6]. In this approach, the interfaces evolve to minimize a thermodynamic potential of the system. Finally, grain growth (GG) and ReX can also be modelled using a level-set (LS) description of the interfaces in the context of uniform grids with a finite difference formulation [7] or in a finite element (FE) framework [8, 9, 10, 11, 12] which is the method used in this paper.

# 2 Level-set method

## 2.1 Representation of the grain boundaries network

As mentioned above, the model considered in this paper works around a LS description of the interfaces in a FE framework. First, grain interfaces are virtually generated either by the Voronoï method or Laguerre-Voronoï method. The Voronoï method consists in generating a diagram composed of a set of $N$ Voronoï nuclei $(S_\mathrm{i})$. Then, a single Voronoï cells $V_\mathrm{i}$ per nucleus is defined following this rule : each Voronoï cell is composed of all points closer to $S_\mathrm{i}$ than to any other nuclei. However, the grain size distribution in the microstructure cannot be *a priori* respected with the Voronoï tessellation method. Thus, a second method called Laguerre-Voronoï can be used. This method consists in generating a diagram where the locations of the cells faces are constrained by a given non-intersecting spherical packing. Thus, the diagram is composed of $N$ seeds each with a weight ($S_\mathrm{i}$,$r_\mathrm{i}$). Then, a single Laguerre-Voronoï $L_\mathrm{i}$ is created per seed following this new rule : each Laguerre-Voronoï cell is composed of all points closer to $S_\mathrm{i}$, via the power distance, than to any other nuclei. Where the power distance from $S_\mathrm{i}$ to x is defined by $d(x,S_\mathrm{i})^2 - r_\mathrm{i}^2$.

The virtual interfaces are then immersed into a FE mesh thanks to LS functions. A LS function $\psi$ is defined over a domain $\Omega$ as the signed distance function to the interface $\Gamma$ of a sub-domain G of $\Omega$. The values of $\psi$ are calculated at each interpolation point (node in the considered P1 formulation) and the sign convention states $\psi \geq 0$ inside G and $\psi \leq 0$ outside :

$$\begin{cases} \psi(x,t) = \pm d(x,\Gamma), x \in \Omega, \\ \Gamma(t) = \{x \in \Omega, \psi(x,t) = 0\}, \end{cases} \tag{1}$$

where d(.,.) corresponds to the Euclidean distance.

## 2.2 Grain boundary kinetic

During a process at high temperature, grain interfaces migrate due to different thermally activated mechanisms. To simulate these mechanisms, each LS interface is displaced during simulation according to a given velocity field $\vec{v}$ by solving a transport equation :

$$\begin{cases} \dfrac{\partial \psi(x,t)}{\partial t} + \vec{v}.\vec{\nabla}\psi(x,t) = 0, \\ \psi(x,t=0) = \psi^0(x), \end{cases} \tag{2}$$

The velocity is assumed to be the contribution of two terms :

$$\vec{v} = \vec{v}_\mathrm{gg} + \vec{v}_\mathrm{e}. \tag{3}$$

$\vec{v}_\mathrm{gg}$ and $\vec{v}_\mathrm{e}$ are respectively the velocities due to capillarity effects and stored energy gradients expressed as follow :

$$\vec{v}_\mathrm{e} = M_\mathrm{b} \Delta E \nabla \psi, \tag{4}$$

$$\vec{v}_\mathrm{gg} = -M_\mathrm{b} \gamma \Delta \psi \nabla \psi, \tag{5}$$

where $M_\mathrm{b}$ is the grain boundary mobility, $\Delta E$ is the stored energy gradient across the interface, and $\gamma$ is the grain boundary energy. These descriptions of the different kinetic terms are correct if and only if the LS function $\psi$ is a distance function ( i.e. $||\nabla\psi|| = 1$) at least in a thin layer $\pm\varepsilon$ around the interface.

The grain boundary mobility $M_\mathrm{b}$, appearing in Eqs. 4 and 5 can be written as a function of temperature :

$$M_\mathrm{b} = M_0 \exp\left(\frac{-Q_\mathrm{m}}{RT}\right), \tag{6}$$

where $Q_m$ is the activation energy for grain boundary migration, $M_0$ is the pre-exponential factor (which can be considered constant at high temperature for the considered 304L material) and $R$ is the gas constant. $M_b$ and $\gamma_b$ are finally assumed constant for all boundaries in the microstructure.

Generally, the number of level-set functions $N$ is taken equal to the number of grains $N_g$ in the microstructure ($N = N_g$). To limit the number of level-set functions and thus the computational cost, a colouring technique has recently been developed and applied in this model [10] leading to a number of LS functions significantly lower than the number of grains ($N \ll N_g$). Finally, Eqs. 2, 4 and 5 of the $N$ level-set functions can be rewritten as convective-diffusive equations :

$$\begin{cases} \dfrac{\partial \psi_i(x,t)}{\partial t} - M\gamma\Delta\psi_i(x,t) + \vec{v}_e.\vec{\nabla}\psi_i(x,t) = 0, \quad \forall i \in \{1,...,N\} \\ \psi_i(x,t=0) = \psi_i^0(x), \end{cases} \tag{7}$$

The interface of every grain of the level-set $\psi_i$ is thus implicitly given at each time step by the equation $\psi_i(t,x) = 0$. Then, the distance functions have to be reinitialized. Indeed, even if the LS functions are initialized as distance functions, their metric properties are not preserved during the resolution of Eq. 7. In order to reinitialize the metric properties of the LS functions, a new direct reinitialization method proposed in [13] is used. This parallel and optimized approach has been proven to be as accurate as a classical direct reinitialization method, while being up to 20 times faster.

Figure 1 presents the initial and final stages of a full field grain growth simulation performed on the austenitic stain steel 304L. The temperature of treatment is 1050°C and the duration of treatment is 5h. The number of initial grains is 8000 while the final number of grains is around 1500. The number of mesh elements is 25M.

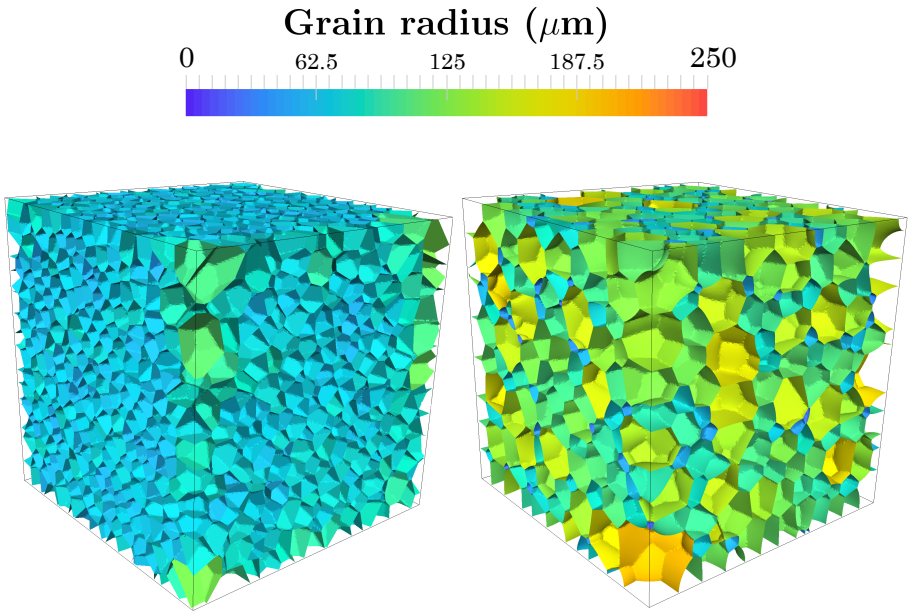


FIGURE 1 – Grain boundaries networks of austenitic stainless steel 304L during a full field grain growth simulation. The initial (left) and final (right) stages corresponding to the instants t=0 and t=5h of the heat treatment are represented. The color code corresponds to the equivalent sphere radius of each grain.

# 3 Dynamic recrystallization modelling

## 3.1 Strain hardening and recovery mechanisms

During inelastic deformation, some dislocations appear in the microstructure due to the strain hardening mechanism, resulting in an increase of the stored energy. However, a part of dislocations can also

disappear by annihilation leading to the recovery mechanism. The strain hardening and recovery mechanisms appearing during deformation, can be modelled at different scales as at a local scale with crystal plasticity models [14, 15, 16] or at a macroscopic scale with mean field laws [17, 18]. In this model, mean field laws are considered to limit the computational cost of the 3D simulations. The Representative Volume Element (RVE) is deformed thanks to a Lagrangian displacement of mesh nodes and an isotropic remeshing operation is performed every 20% of deformation. The described full-field method is then used for modelling microstructure and grain boundary migration during deformation.

A dislocation density field is defined constant per grain at the beginning of the simulation. Considering $j$ grains in the microstructure, the averaged dislocation density field in each grain $j$ noted $\langle\rho_{\mathrm{j}}\rangle$ is assumed to evolve according to the Yoshie-Lasraoui-Jonas law :

$$\dot{\langle\rho_{\mathrm{j}}\rangle} = \left(K_1 - K_2\langle\rho_{\mathrm{j}}\rangle\right)\dot{\varepsilon}^{\mathrm{p}}_{\mathrm{eff}}, \tag{8}$$

where $\dot{\varepsilon}^{\mathrm{p}}_{\mathrm{eff}}$ denotes the rate of the effective plastic strain, $\mathrm{K_1}$ and $\mathrm{K_2}$ are two constants which represent respectively the strain hardening and recovery term. A superposed dot denotes differentiation with respect to time. At each time increment, this differential equation is solved with an explicit Euler method, i.e.

$$\frac{\langle\rho_{\mathrm{j}}\rangle^{(\mathrm{t}+\Delta\mathrm{t})} - \langle\rho_{\mathrm{j}}\rangle^{\mathrm{t}}}{\Delta\varepsilon} = K_1 - K_2\langle\rho_{\mathrm{j}}\rangle^{\mathrm{t}}, \tag{9}$$

leading to the final equation :

$$\langle\rho_{\mathrm{j}}\rangle^{(\mathrm{t}+\Delta\mathrm{t})} = K_1\Delta\varepsilon + (1 - K_2\Delta\varepsilon)\langle\rho_{\mathrm{j}}\rangle^{\mathrm{t}}. \tag{10}$$

When a grain boundary migrates, the swept area is almost free of defects, i.e. dislocations free. This phenomenon of "recovery per boundary migration" can be described by a decrease of the dislocation density in growing grains. Thus, during boundary migration, a minimal dislocation density equal to $\rho_0$, which is material dependant, is attributed to swept areas. Then the new dislocation density is averaged in each grain following the equation :

$$\langle\rho_{\mathrm{j}}\rangle^{(\mathrm{t}+\Delta\mathrm{t})}V^{(\mathrm{t}+\Delta\mathrm{t})} = \langle\rho_{\mathrm{j}}\rangle^{\mathrm{t}}V^{\mathrm{t}} + dV\rho_0, \tag{11}$$

where dV represents the swept volume between the instants t and t+$\Delta$t, and $\rho_0$ is the low value of dislocation density attributed to the swept areas, usually taken as $1.10^{11}$ $\mathrm{m}^{-2}$ for the 304L steel.

The flow stress $\sigma_{\mathrm{i}}$ in the $\mathrm{i}^{th}$ grain is computed during deformation from its average dislocation density $\rho_{\mathrm{i}}$ using the Taylor equation :

$$\sigma_{\mathrm{i}} = \sigma_0 + M\alpha\mu b\sqrt{\langle\rho_{\mathrm{i}}\rangle}, \tag{12}$$

where $\sigma_0$ is a "dislocations-free" yield stress, $M$ is the Taylor factor and $\alpha$ is a constant set to 0.2. Then the total flow stress $\langle\sigma\rangle$ is calculated as a volumic averaged of the flow stresses of every grains :

$$\langle\sigma\rangle = \frac{\sum\sigma_i V_i}{V_{\mathrm{tot}}}, \tag{13}$$

The PDRX mechanism is simply considered after deformation by modelling the migration of grain boundaries given by Eqs. 3, 4 and 5, the recovery per boundary migration given by Eq. 11 and the recovery per annihilation of dislocation given by Eq. 14 :

$$\dot{\langle\rho_{\mathrm{j}}\rangle} = -K_{\mathrm{s}}\langle\rho_{\mathrm{j}}\rangle, \tag{14}$$

We consider that no nucleation of new grains occurs during PDRX.

### 3.2 Nucleation mechanism

When enough energy is accumulated in the material due to plastic deformation, some dislocation networks can develop within certain grains and tend to the formation of substructures, mainly located at

grain boundaries [19]. Different criteria need to be verified locally in order that a substructure becomes a nucleus : a mobile high-angle grain boundary has to be formed by the nucleation event and a high stored energy gradient across the interface must be involved in order to provide enough positive driving pressure for growth. In the considered framework, $\gamma$ is assumed constant and thus only the stored energy is taken into account. The nucleation mechanism appearing during hot deformation is taken into account in this model following a mean-field approach used in [20] that is composed of two parts. First, new grains are assumed to nucleate only if the strain reaches a critical value, which valid the second criterion mentioned previously. This critical strain is equivalent to a critical value of dislocation density noted $\rho_{\mathrm{cr}}$ and is initially calculated according to the equation :

$$\rho_{\mathrm{cr}} = \left( \frac{20 K_1 \gamma_{\mathrm{b}} \dot{\varepsilon}^{\mathrm{p}}_{\mathrm{eff}}}{3 M_{\mathrm{b}} \tau^2} \right)^{(1/3)}, \tag{15}$$

where $\tau = \mu b^2/2$ is the dislocation line energy. The influence of the temperature and strain rate on $\rho_{\mathrm{cr}}$ is taken into account in Eq. 15 by the parameters $K_1$, $\dot{\varepsilon}^{\mathrm{p}}_{\mathrm{eff}}$ and $M_{\mathrm{b}}$. It is physically assumed that $\rho_{\mathrm{cr}}$ increases when decreasing temperature or increasing strain rate. As the dynamic recovery mechanism is neglected in Eq. 15, this latter can be inaccurate in many cases. Thus, the equation proposed in [20] and taking the dynamic recovery mechanism into account has been implemented in our model :

$$\rho_{\mathrm{cr}} = \left[ \frac{-2\gamma_{\mathrm{b}} \dot{\varepsilon}^{\mathrm{p}}_{\mathrm{eff}} \dfrac{K_2}{M_{\mathrm{b}} \tau^2}}{\ln\left(1 - \dfrac{K_2}{K_1}\rho_{\mathrm{cr}}\right)} \right]^{1/2}. \tag{16}$$

To summarize, an initial value of $\rho_{cr}$ is calculated according to Eq. 15 and an iterative calculation using Eq. 16 leads to a converged value of $\rho_{\mathrm{cr}}$ that is used in our model.

Once a grain reaches the critical dislocation density $\rho_{\mathrm{cr}}$, the nucleation rate $\dot{N}$ is calculated according to the proportional nucleation model of Peczak and Luton [21] :

$$\dot{N} = K_{\mathrm{g}} S_{\mathrm{b}} \Delta \mathrm{t}, \tag{17}$$

where $K_{\mathrm{g}}$ is a probability coefficient related to the thermo-mechanical conditions, i.e. the temperature and the effective plastic strain rate, $S_{\mathrm{b}}$ is the total grain boundary area of grains verifying $\rho_{\mathrm{i}} > \rho_{\mathrm{cr}}$.

When a new nucleus appears in the microstructure, its initial radius must be high enough to counter the capillarity forces. This corresponds to the condition when the stored energy of the material is large enough to overcome the capillary force of the nucleus (Bailey-Hirsch),

$$r^* = \omega \frac{2\gamma_{\mathrm{b}}}{\rho_{\mathrm{cr}} \tau}, \tag{18}$$

where $\omega > 1$ is a factor ensuring that the created nucleus has a required driving force for growth.

The nucleus can grow in the microstructure by consuming the surrounding worked grains. The velocity of migrating boundaries are described following Eqs. 3, 4 and 5.

To illustrate results obtained with the proposed DRX-PDRX model, a simulation has been launched for 304L at a temperature of 1000°C and a strain rate of $0.01\mathrm{s}^{-1}$. The REV is firstly deformed during 100s following by a 30min hold at 1000°C. Several screenshots illustrating the REV at four different instants of the simulation are presented on Fig. 2.

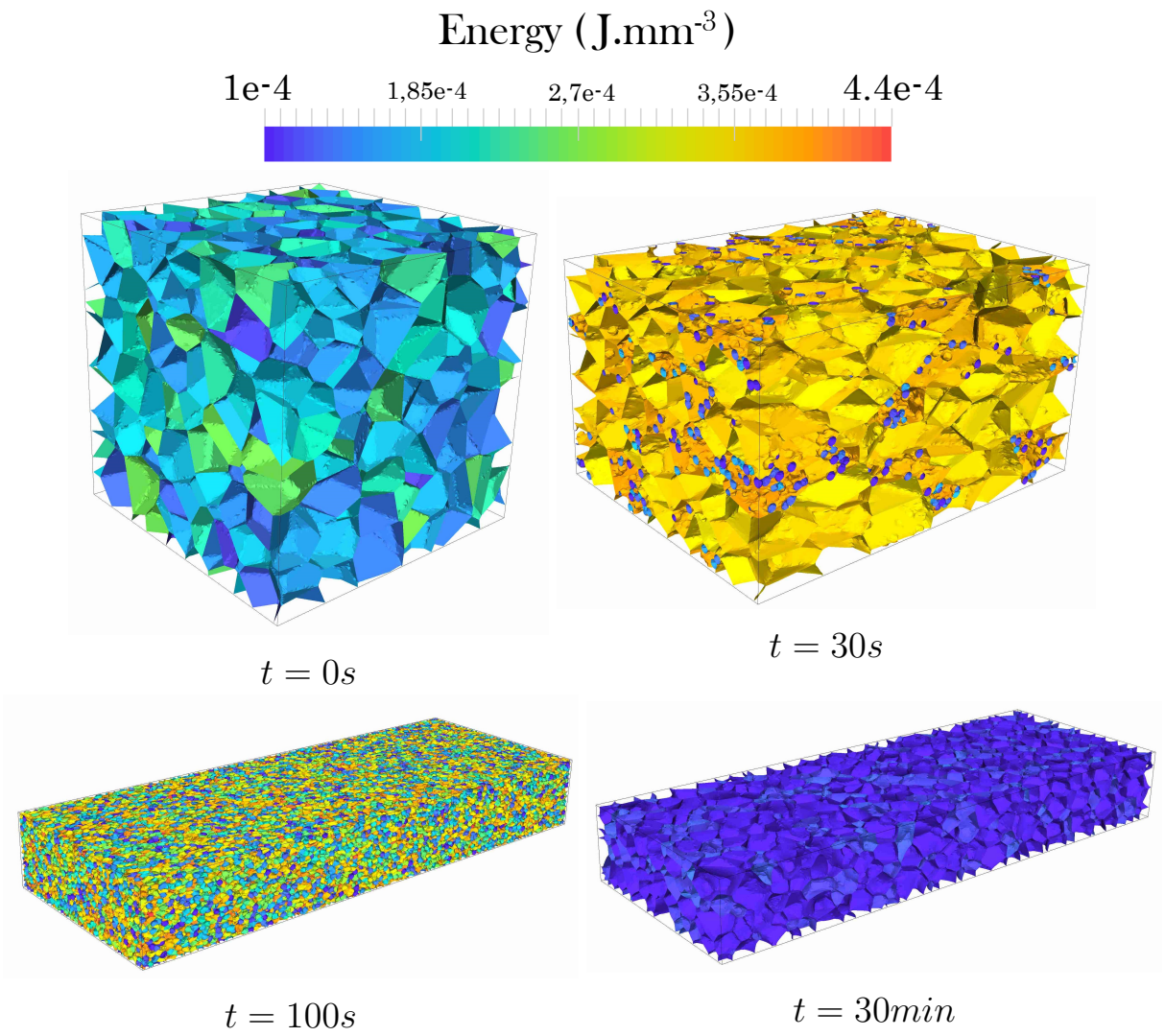


FIGURE 2 – A DRX+PDRX simulation at large deformation for a 304L austenitic stainless steel . The REV is firstly deformed at 1000°C during 100s following by a 1000°C hold during 30min.

## 4 Conclusion

In the present work, a 3D model based on the level-set method in a finite element framework has been presented to model the DRX and PDRX phenomena in austenitic stainless steel 304L at large deformations. The first part was dedicated to the presentation of the level-set method while the second part was focused on the mean field governing equations. A 3D illustrating case of the DRX + PDRX mechanisms at very large deformation has been finally presented. It was concluded that the level-set approach coupled to a remesher provides an accurate method to capture the interfaces (i.e. grain boundaries) all along the simulation while mean field laws using for the nucleation, work hardening and recovery mechanisms lead to relatively low computational costs. Future investigations will aim to perform a sensitivity study of the input parameters, to calibrate more finely the model parameters according to experimental investigations and finally validate this full field formalism thanks to the experimental results.

## Acknowledgements

The supports of the French Agence Nationale de la Recherche (ANR), ArcelorMittal, AREVA, ASCOMETAL, AUBERT&DUVAL, CEA, SAFRAN through the DIGIMU Industrial Chair and consortium are gratefully acknowledged.

## Références


[1] H. Hallberg. Approaches to Modeling of Recrystallization. *Metals*, 1(1) :16–48, 2011.

[2] A. D. Rollett. Overview of modeling and simulation of recrystallization. *Progress in Materials Science*, 42(1-4) :79–99, 1997.

[3] A. D. Rollett and D. Raabe. A hybrid model for mesoscopic simulation of recrystallization. *Computational Materials Science*, 21(1) :69–78, 2001.

[4] D. Raabe. Introduction of a scalable three-dimensional cellular automaton with a probabilistic switching rule for the discrete mesoscale simulation of recrystallization phenomena. *Philosophical Magazine A*, 79(10) :2339–2358, oct 1999.

[5] L.A. Barrales Mora, G. Gottstein, and L.S. Shvindlerman. Three-dimensional grain growth : Analytical approaches and computer simulations. *Acta Materialia*, 56(20) :5915–5926, 2008.

[6] C.E. Krill and L.Q. Chen. Computer simulation of 3-D grain growth using a phase-field model. *Acta Materialia*, 50(12) :3059–3075, 2002.

[7] M. Elsey, S. Esedoglu, and P. Smereka. Diffusion generated motion for grain growth in two and three dimensions. *Journal of Computational Physics*, 228(21) :8015–8033, 2009.

[8] M. Bernacki, Y. Chastel, T. Coupez, and R.E. Logé. Level set framework for the numerical modelling of primary recrystallization in polycrystalline materials. *Scripta Materialia*, 58(12) :1129–1132, 2008.

[9] M. Bernacki, R.E. Logé, and T. Coupez. Level set framework for the finite-element modelling of recrystallization and grain growth in polycrystalline materials. *Scripta Materialia*, 64(6) :525–528, 2011.

[10] B. Scholtes, M. Shakoor, A. Settefrati, P.-O. Bouchard, N. Bozzolo, and M. Bernacki. New finite element developments for the full field modeling of microstructural evolutions using the level-set method. *Computational Materials Science*, 109 :388–398, 2015.

[11] A. Agnoli, N. Bozzolo, R. Logé, J.-M. Franchet, J. Laigo, and M. Bernacki. Development of a level set methodology to simulate grain growth in the presence of real secondary phase particles and stored energy – Application to a nickel-base superalloy. *Computational Materials Science*, 89 :233–241, 2014.

[12] B. Scholtes, R. Boulais-sinou, A. Settefrati, D. Pino Muñoz, I. Poitrault, A. Montouchet, N. Bozzolo, and M. Bernacki. 3D level set modeling of static recrystallization considering stored energy fields. *Computational Materials Science*, 122 :57–71, 2016.

[13] M. Shakoor, B. Scholtes, P.-O. Bouchard, and M. Bernacki. An efficient and parallel level set reinitialization method – Application to micromechanics and microstructural evolutions. *Applied Mathematical Modelling*, 39(23-24) :7291–7302, 2015.

[14] Y. Mellbin, H. Hallberg, and M. Ristinmaa. A combined crystal plasticity and graph-based vertex model of dynamic recrystallization at large deformations. *Modelling and Simulation in Materials Science and Engineering*, 23(4) :045011, 2015.

[15] E. Popova, Y. Staraselski, A. Brahme, R. K. Mishra, and K. Inal. Coupled crystal plasticity - Probabilistic cellular automata approach to model dynamic recrystallization in magnesium alloys. *International Journal of Plasticity*, 66 :85–102, 2015.

[16] L. Chen, J. Chen, R. A. Lebensohn, Y. Z. Ji, T. W. Heo, S. Bhattacharyya, K. Chang, S. Mathaudhu, Z. K. Liu, and L. Q. Chen. An integrated fast Fourier transform-based phase-field and crystal plasticity approach to model recrystallization of three dimensional polycrystals. *Computer Methods in Applied Mechanics and Engineering*, 285 :829–848, 2015.

[17] U. F. Kocks. Laws for Work-Hardening and Low-Temperature Creep. *Journal of Engineering Materials and Technology*, 98(1) :76, 1976.

[18] H. Mecking and U.F. Kocks. Kinetics of flow and strain-hardening. *Acta Metallurgica*, 29(11) :1865–1875, 1981.

[19] F. J. Humphreys and M. Hatherly. *Recrystallization and related annealing phenomena*. Elsevier, 2004.

[20] O. Beltran, K. Huang, and R.E. Logé. A mean field model of dynamic and post-dynamic recrystallization predicting kinetics, grain size and flow stress. *Computational Materials Science*, 102 :293–303, 2015.

[21] P. Peczak and M. J. Luton. The effect of nucleation models on dynamic recrystallization I. Homogeneous stored energy distribution. *Philosophical Magazine Part B*, 68(1) :115–144, 1993.